

# Applications of Mathematics

---

Tomáš Bayer; Milada Kočandrlová

Reconstruction of map projection, its inverse and re-projection

*Applications of Mathematics*, Vol. 63 (2018), No. 4, 455–481

Persistent URL: <http://dml.cz/dmlcz/147321>

## Terms of use:

© Institute of Mathematics AS CR, 2018

Institute of Mathematics of the Czech Academy of Sciences provides access to digitized documents strictly for personal use. Each copy of any part of this document must contain these *Terms of use*.



This document has been digitized, optimized for electronic delivery and stamped with digital signature within the project *DML-CZ: The Czech Digital Mathematics Library* <http://dml.cz>

## RECONSTRUCTION OF MAP PROJECTION, ITS INVERSE AND RE-PROJECTION

TOMÁŠ BAYER, MILADA KOČANDRLOVÁ, Praha

Received March 31, 2018. Published online July 20, 2018.

*Abstract.* This paper focuses on the automatic recognition of map projection, its inverse and re-projection. Our analysis leads to the unconstrained optimization solved by the hybrid BFGS nonlinear least squares technique. The objective function is represented by the squared sum of the residuals. For the map re-projection the partial differential equations of the inverse transformation are derived. They can be applied to any map projection. Illustrative examples of the stereographic and globular Nicolosi projections frequently used in early maps are involved and their inverse formulas are presented.

*Keywords:* mathematical cartography; inverse projection; analysis; nonlinear least squares; partial differential equation; optimization; hybrid BFGS; early map; re-projection

*MSC 2010:* 34B16, 34C25

### 1. INTRODUCTION

Mathematical cartography concerns the wider aspect of the spherical representation of the curved Earth surface on a flat map. There is a long history of using various types of map projections, progressing from simple geometric constructions to more complex variants. Early attempts are mostly connected with Ancient Greece, where geometry, cartography, and geography were among the primary interests of many researchers. Recall the earliest conical projection associated with Claudius Ptolemy and his famous second world map, or the stereographic projection first used by Hipparchus. At that time, map projections had a geometric justification. The development of the natural sciences, together with the rise of calculus, caused a significant acceleration in the proposal of new map projections. A few hundred map projections have been described since the Ancient Greece era. For map construction, only approximately 30 of them have been applied.

Due to the different curvatures of both surfaces, length, aerial or angular distortions affecting the map geometry appear. There is no isometry mapping between points on the sphere  $\mathbb{S}^2$  and the plane  $\sigma$ . Working with multiple maps in different map projections, it is necessary to unify their map projection in accordance with the current standards given by the national grids (obligatory for different states) or using more appropriate map projection in terms of distortions. In other words, a transformation of the source map projection to the destination projection needs to be undertaken. This process, called *re-projecton*, assigns spatial information to each map element so that the corresponding content of different maps is well-aligned, one above the other in a coordinate system of the destination projection. Unfortunately, many maps lack the information about the projection given by the set of constants. Hence, there is a need to perform a mathematical analysis and reconstruction of map projection and use it to find its inverse form. The input data are represented by the sets of points  $P$ ,  $Q$  on the analyzed map and on the sphere.

From the mathematical point of view this task leads to unconstrained optimization. So far, the parameters have been estimated only visually, without any deeper theoretical background, which has led to many mistakes. The proposed technique based on the hybrid BFGS method seems to be efficient, especially for the nonlinear least squares; only a few iterations are required for most projections. Another solution using differential evolution can be found in [4], the simplex method approach in [3].

During the analysis, the unknown projection is classified (projection family, projection name), its constant values as well as the map parameters (scale, rotation) are estimated. In some cases the task is ill-conditioned, for early maps with a lack of a solid geometric basis it leads to a large-residual problem. For most cases, the solution can be found in reasonable time.

Finding the projection inverse led to partial differential equations of the coordinate functions derived from the local linear scales. Its algebraic solution is relatively complicated, a numerical solution (Newton-Raphson method) or approximation (Laurent series) is required.

Section 3 describes the map projection and its parameters. Section 4 deals with projection analysis. Derivations of the partial differential equations of inverse transformation are described in Section 5. All the above-mentioned methods have been implemented in the new software `detectproj` written in Java available under a GNU/GPL2 license.

## 2. RELATED WORK

The theoretical backgrounds of the map projection analysis are described in [26], [27]. Measuring the map projection similarity using the residuals of the corresponding points was introduced in [28]. A technique based on the Nelder-Mead optimization of the corresponding 0D-2D features can be found in [3], the nonlinear least squares and differential evolution solutions in [4]. Another method using the decision trees was presented in [2]. The mathematical reconstruction of the projection graticule (represented by the set of meridians and parallels) involving singularities has been described in [6]. There are some software tools for the projection analysis, for example: `prjfinder` [10], `MapAnalyst` [16], `detectproj` [5]. The inverse form of map projections has been studied in many papers. The numerical methods based on the inverse Jacobian matrix can be found in [15], and general transformations in [30], [7], [8]. Inverse methods for families of pseudocylindrical projections are described in [14], for the Robinson projection [21], for the Mollweide projection [17], for the Snyder polyhedral projection [12] and for projections derived from Lambert azimuthal in [22]. The inverse projection equations are published in several books, for example in [24], [25], [9], [30].

## 3. MAP PROJECTION AND ITS DETERMINED PARAMETERS

Without loss of precision, each map projection transforms a curved surface (i.e. reference surface) into a flat surface (i.e. projected surface). Let the sphere  $\mathbb{S}^2 \subset \mathbb{R}^3$  with the radius  $R$  be centered at the origin of the Cartesian coordinate system, let the local coordinate system  $\{\varphi, \lambda\}$ -spherical latitude and longitude be the reference surface, and let the plane  $\sigma$  with the Cartesian coordinate system  $\{X, Y\}$  be the projected surface. Since there is no isometric projection of the sphere in  $\mathbb{R}^3$  (or its parts) into plane, map projections used in cartography meet several requirements. Let us summarize their basic properties.

**Definition 3.1.** Projection of the set  $M = \langle -\pi/2, \pi/2 \rangle \times \langle -\pi, \pi \rangle$  into  $\mathbb{R}^2$ , given by the equations  $X = F(\varphi, \lambda)$ ,  $Y = G(\varphi, \lambda)$ , is called the map projection  $\mathbb{P}$  of the sphere  $\mathbb{S}^2$  into the plane  $\sigma$ . Here  $F$  and  $G$  are real measurable functions defined on  $M$ .

**Remark 3.2.** Every point  $Q$  of the sphere is associated with an ordered pair of local coordinates  $[\varphi, \lambda] \in M$ .

**Definition 3.3.** A projection  $\mathbb{P}: \mathbb{S}^2 \rightarrow \sigma$  is called to be continuous at the point  $Q = [\varphi, \lambda]$  if the coordinate functions  $F, G$  are continuous at  $Q$ .

**Definition 3.4.** Projection  $\mathbb{P}: \mathbb{S}^2 \rightarrow \sigma$  is injective on the set  $M$  if for any different points  $Q_1, Q_2 \in \mathbb{S}^2$  we have  $\mathbb{P}(Q_1) \neq \mathbb{P}(Q_2)$ .

**Definition 3.5.** Projection  $\mathbb{P}$  is nonsingular on a domain  $\Omega \subset M$  if the first derivatives of  $F, G$  are continuous on  $\Omega$  and the Jacobian matrix determinant is nonzero.

**Remark 3.6.** According to Definition 3.5 the projection  $\mathbb{P}$  is continuous on the domain  $\Omega$ .

**Theorem 3.7.** *If the projection  $\mathbb{P}$  on the boundary of  $Q$  is nonsingular, then the inverse projection  $\mathbb{P}^{-1}$  is nonsingular on the boundary of  $\mathbb{P}(Q)$  and the Jacobians of both projections are reciprocal.*

**Remark 3.8.** Apparently, the projection  $\mathbb{P}$  will still be nonsingular if instead of the closed interval  $M$  an open interval  $M = (-\pi/2, \pi/2) \times (-\pi, \pi)$  will be considered. From the sphere  $\mathbb{S}^2$ , the Northern and Southern Poles  $A = [\pi/2, 0]$  and  $B = [-\pi/2, 0]$  will be removed, since they are singular due to the parameterization  $\{\varphi, \lambda\}$  as well as one meridian.

Map projections are proposed to represent the entire Earth surface, its hemisphere, a continent, or a country as accurately as possible. To avoid distortions, the central point of the projected territory is selected as a point of touch of the plane  $\sigma$  and the sphere  $\mathbb{S}^2$ . This point, denoted by  $K = [\varphi_K, \lambda_K]$ , represents *the cartographic pole* with the local coordinate system  $\{\varphi', \lambda'\}$ .

**Remark 3.9.** From the sphere  $\mathbb{S}^2$ , the cartographic pole  $K = [\pi/2, 0]$  and its opposite point  $L = [-\pi/2, 0]$  will be removed since they are singular due to the parameterization  $\{\varphi', \lambda'\}$ .

The relationship between the spherical coordinate systems  $\{\varphi, \lambda\}$  and  $\{\varphi', \lambda'\}$  can be found using the law of sines and five-part rules ([23], p. 10) from the spherical triangle  $AKQ$ , where  $\Delta\lambda = \lambda - \lambda_K$  (see Fig. 3.1):

$$\begin{aligned} \sin \lambda' &= \frac{\cos \varphi \sin \Delta\lambda}{\cos \varphi'}, & \cos \lambda' &= \frac{\cos \varphi \sin \varphi_K \cos \Delta\lambda - \sin \varphi \cos \varphi_K}{\cos \varphi'}, \\ \sin \Delta\lambda &= \frac{\cos \varphi' \sin \lambda'}{\cos \varphi}, & \cos \Delta\lambda &= \frac{\sin \varphi' \cos \varphi_K + \cos \varphi' \sin \varphi_K \cos \lambda'}{\cos \varphi}. \end{aligned}$$

This leads to the following theorem.

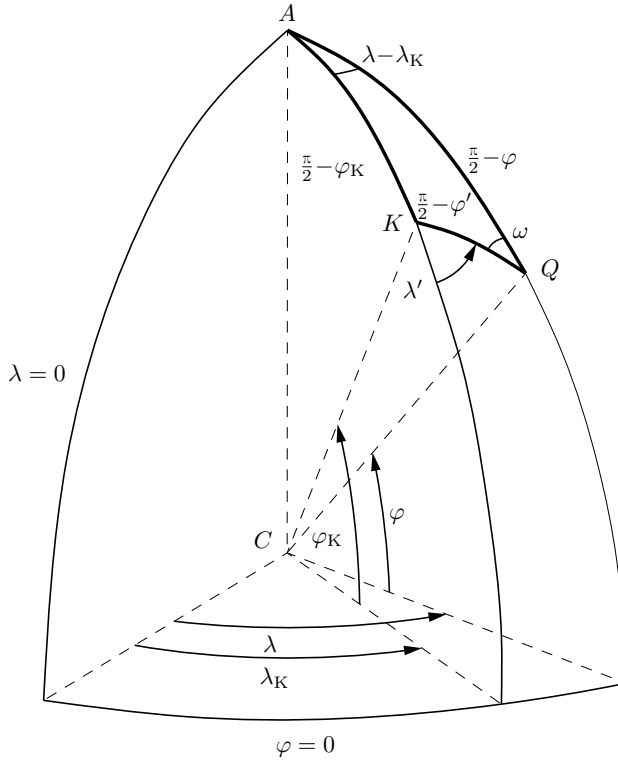


Figure 3.1. Oblique aspect of the map projection, cartographic pole  $K = [\varphi_K, \lambda_K]$ .

**Theorem 3.10.** For local coordinate systems  $\{\varphi, \lambda\}$  and  $\{\varphi', \lambda'\}$  on the sphere  $\mathbb{S}^2$  the coordinate transformation between the normal and oblique aspects is

$$(3.1) \quad \sin \varphi' = \sin \varphi_K \sin \varphi + \cos \varphi_K \cos \varphi \cos \Delta\lambda,$$

$$(3.2) \quad \tan \lambda' = \frac{\cos \varphi \sin \Delta\lambda}{\cos \varphi \sin \varphi_K \cos \Delta\lambda - \sin \varphi \cos \varphi_K}.$$

The inverse transformation is

$$\begin{aligned} \sin \varphi &= \sin \varphi_K \sin \varphi' - \cos \varphi_K \cos \varphi' \cos \lambda', \\ \tan \Delta\lambda &= \frac{\cos \varphi' \sin \lambda'}{\cos \varphi' \sin \varphi_K \cos \lambda' + \sin \varphi' \cos \varphi_K}. \end{aligned}$$

The spherical coordinates of  $Q \in \mathbb{S}^2$  are a function of  $\varphi_K, \lambda_K$ :

$$\begin{aligned} [\varphi'(\varphi_K, \lambda_K), \lambda'(\varphi_K, \lambda_K)] &= [H(\varphi, \lambda), I(\varphi, \lambda)], \\ [\varphi(\varphi_K, \lambda_K), \lambda(\varphi_K, \lambda_K)] &= [H^{-1}(\varphi', \lambda'), I^{-1}(\varphi', \lambda')]. \end{aligned}$$

**3.1. Determined parameters.** The map projection  $\mathbb{P}$  is described by 6 parameters, and the other 4 refer to the analyzed map. Considering a reduction to the centroids of both sets  $P, P'$ , the total amount of the determined parameters decreases to 8.

**Parameters of the map projection.** During the analysis, the following constants of the projection  $\mathbb{P}$  affecting the graticule shape are determined:

▷ *Cartographic pole*  $K = [\varphi_K, \lambda_K]$

This factor has a crucial influence on the shape of the graticule.

▷ *True parallels*  $\varphi_1, \varphi_2$

Conic projections in the secant form specify true parallels  $\varphi_1, \varphi_2, \varphi_1 \neq \varphi_2$ , for the tangent form it is  $\varphi_1 = \varphi_2$ . For cylindrical projections in the secant form it is  $\varphi_1 = -\varphi_2$ , the tangent form brings  $\varphi_1 = \varphi_2 = 0$ . For the remaining map projections it is  $\varphi_1 = \varphi_2$ , but some of them do not use true parallels. In the oblique aspect of the projection,  $\varphi'_1, \varphi'_2$  are determined instead of  $\varphi_1, \varphi_2$ .

▷ *Longitude*  $\lambda_0$  *of the central meridian*

To minimize the distortion and provide a true depiction of the mapped region, the central meridian is shifted by  $\lambda_0$ , for the oblique aspect by  $\lambda'_0$ .

▷ *Arbitrary parameter*  $\kappa$

This may represent any constant value of the projection. Describing the distance of the center of the projection from the sphere  $\mathbb{S}^2$  center it is widely used for perspective projections.

**Parameters of the map.** The analysis process should be partially or fully invariant to the values of the map constants that do not affect the graticule shape.

▷ *Radius of the auxiliary sphere*  $R'$

The analyzed map represents a reduced-scale model associated with the radius  $R'$  of the auxiliary sphere.

▷ *Shifts*  $\Delta X, \Delta Y$

The analyzed map may utilize additional shifts  $\Delta X, \Delta Y$ , which is typical for some projections. Let us mention UTM (Universal Transverse Mercator)—the Mercator projection in the transverse aspect with the planisphere divided into 60 zones, each  $6^\circ$  of longitude in width, used for military maps, where  $\Delta X = 0, \Delta Y = 500\,000$  m.

▷ *Angle of rotation*  $\alpha$

This corrects the additional rotation of the map caused by the inappropriate digitization or a switched orientation of the page (portrait vs landscape).

The coordinates of the point  $P_i = [X_i, Y_i] \in \sigma$  representing the image of  $Q_i = [\varphi_i, \lambda_i] \in \mathbb{S}^2$  can be written as a function of the determined parameters. For the

normal aspect of the projection ( $K = A$ ) the coordinate functions have the form of

$$\begin{aligned} X_i(R', \varphi_1, \varphi_2, \lambda_0, \Delta X) &= F(\varphi_i, \lambda_i), \\ Y_i(R', \varphi_1, \varphi_2, \lambda_0, \Delta Y) &= G(\varphi_i, \lambda_i). \end{aligned}$$

In the transverse/oblique aspect of the projection they can be written as

$$\begin{aligned} X_i(R', \varphi_K, \lambda_K, \varphi'_1, \varphi'_2, \lambda'_0, \Delta X) &= F(H(\varphi_i, \lambda_i), I(\varphi_i, \lambda_i)), \\ Y_i(R', \varphi_K, \lambda_K, \varphi'_1, \varphi'_2, \lambda'_0, \Delta Y) &= G(H(\varphi_i, \lambda_i), I(\varphi_i, \lambda_i)). \end{aligned}$$

In the case of the rotation equivariance, the coordinate functions have a more complex form, see Section 4.

#### 4. ANALYSIS OF THE MAP PROJECTION

The input data for the projection analysis are represented by the identical points on the analyzed map and on the sphere (or on the reference map).

**Proposition 4.1.** *Let  $Q = \{Q_1, \dots, Q_n\}$ ,  $n \in \mathbb{N}$ , be a set of points on the sphere  $\mathbb{S}^2$  and  $P = \{P_1, \dots, P_n\}$ ,  $n \in \mathbb{N}$ , be a set of their images on the map (on the plane  $\sigma$ ). Then the projection  $\mathbb{P}_x: \sigma \rightarrow \mathbb{S}^2$  given by the set of parameters  $x^T = (R', \alpha, \varphi_K, \lambda'_K, \varphi'_1, \varphi'_2, \lambda'_0, \kappa, \Delta X, \Delta Y)$  exists such that  $\mathbb{P}_x(P_i) = Q_i$ .*

Furthermore, let us denote by  $P' = \{P'_1, \dots, P'_n\}$ ,  $n \in \mathbb{N}$ , the set of corresponding points measured on the analyzed map and  $r_i(x) = P_i - P'_i$  to be the residual between the image of  $Q_i$  in  $\mathbb{P}_x$  and the analyzed point  $P'_i$ . Depending on the sets  $P'$ ,  $Q$ , the optimal vector  $x$  of the map projection  $\mathbb{P}$  constants is determined. Reducing  $P$ ,  $P'$  to their centers of mass  $C_p$ ,  $C'_p$ , the amount of the determined parameters may decrease to 8. The reduced coordinates are

$$\begin{aligned} P_i - C_p &= (\xi_i, \eta_i) = (X_i - X_c, Y_i - Y_c), \\ P'_i - C'_p &= (\xi'_i, \eta'_i) = (X'_i - X'_c, Y'_i - Y'_c), \end{aligned}$$

where  $(X'_i, Y'_i)$  are coordinates of a point  $P'_i$  on the analyzed map. The determined vector of unknown parameters for the reduced coordinates at iteration  $k$  is written as

$$x_k^T = (R', \alpha, \varphi_K, \lambda_K, \varphi'_1, \varphi'_2, \lambda'_0, \kappa),$$

where the shifts  $\Delta X, \Delta Y$  are evaluated from (4.1). While the last six parameters refer to the map projection  $\mathbb{P}$ , two remaining constants describe the map. In general,

at least 4 identical points are required to determine  $x$ . The coordinates of  $Q_i$  in  $\mathbb{P}_x$  reduced according to the center of mass  $C_p$ , rotated by the angle  $\alpha_k$ , are written as

$$\chi_i(x_k) = q_{1,k}\xi_{i,k} - q_{2,k}\eta_{i,k}, \quad \gamma_i(x_k) = q_{2,k}\xi_{i,k} + q_{1,k}\eta_{i,k},$$

where  $q_{1,k} = \delta_k \cos \alpha_k$ ,  $q_{2,k} = \delta_k \sin \alpha_k$  are scale factors of the Helmert transformation describing the analyzed map. The definition of the residual vector is

$$r(x_k) = \begin{bmatrix} \chi_1(x_k) \\ \vdots \\ \frac{\chi_n(x_k)}{\gamma_1(x_k)} \\ \vdots \\ \gamma_n(x_k) \end{bmatrix} - \begin{bmatrix} \xi'_1 \\ \vdots \\ \xi'_n \\ \eta'_1 \\ \vdots \\ \eta'_n \end{bmatrix} = A_k q_k - l.$$

Unlike the constant values of the projection estimated from the nonlinear least squares iteratively,  $q_{1,k}$  and  $q_{2,k}$  are found as a solution of the associated linear least squares problem

$$\phi(x_k) = \frac{1}{2} r^T(x_k) r(x_k) = (A_k q_k - l)^T (A_k q_k - l) = \min$$

with the condition for minimum  $\partial\phi(x_k)/\partial x_k = A_k^T A_k q_k - A_k^T l = 0$ , where

$$q_k = (A_k^T A_k)^{-1} A_k^T l.$$

The radius  $R'$  of the auxiliary sphere, scale factor  $\delta$ , rotation  $\alpha$ , and map scale  $S$  are

$$R'_k = R_{k-1} \delta_k, \quad \delta_k = \sqrt{q_{1,k}^2 + q_{2,k}^2}, \quad \alpha_k = \arctan \frac{q_{2,k}}{q_{1,k}}, \quad S_k = \frac{i_r}{I} \frac{R}{R'_k},$$

where  $R$  is the Earth radius,  $i_r$  represents the image resolution in DPI, and  $I$  is the length of one inch ( $I = 25.4$  mm). To create an overlay of the analyzed map and its reconstructed graticule, the coordinates  $(X_i, Y_i)$  of the sampled meridian/parallel points need to be reduced

$$\begin{aligned} X''_i &= \chi_i(x_k) + X'_c = q_{1,k} X_{i,k} - q_{2,k} Y_{i,k} + \Delta X_k, \\ Y''_i &= \gamma_i(x_k) + Y'_c = q_{2,k} X_{i,k} + q_{1,k} Y_{i,k} + \Delta Y_k, \end{aligned}$$

the shifts  $\Delta X$ ,  $\Delta Y$  are

$$(4.1) \quad \Delta X_k = X'_c - q_{1,k} X_{c,k} + q_{2,k} Y_{c,k}, \quad \Delta Y_k = Y'_c - q_{2,k} X_{c,k} + q_{1,k} Y_{c,k},$$

see Fig. 4.1. Estimating the values of  $q_{1,k}$ ,  $q_{2,k}$  at once instead of the series of increments at iteration  $k$ , brings a sufficient robustness against the initial guess  $x_0$  as well as a low sensitivity to the discrepant scales of  $P$ ,  $P'$  and the rotation  $\alpha$ . Entries of the Jacobian matrix  $J(x_k)$  are partial derivatives of functions  $\chi_i(x_k)$ ,  $\gamma_i(x_k)$

$$\begin{aligned} \frac{\partial \chi_k}{\partial \cdot}(\varphi_i, \lambda_i) &= \left[ \frac{\partial X_k}{\partial \cdot}(\varphi_i, \lambda_i) - \frac{1}{n} \sum_{l=1}^n \frac{\partial X_k}{\partial \cdot}(\varphi_l, \lambda_l) \right] q_{1,k} \\ &\quad - \left[ \frac{\partial Y_k}{\partial \cdot}(\varphi_i, \lambda_i) - \frac{1}{n} \sum_{l=1}^n \frac{\partial Y_k}{\partial \cdot}(\varphi_l, \lambda_l) \right] q_{2,k}, \\ \frac{\partial \gamma_k}{\partial \cdot}(\varphi_i, \lambda_i) &= \left[ \frac{\partial X_k}{\partial \cdot}(\varphi_i, \lambda_i) - \frac{1}{n} \sum_{l=1}^n \frac{\partial X_k}{\partial \cdot}(\varphi_l, \lambda_l) \right] q_{2,k} \\ &\quad + \left[ \frac{\partial Y_k}{\partial \cdot}(\varphi_i, \lambda_i) - \frac{1}{n} \sum_{l=1}^n \frac{\partial Y_k}{\partial \cdot}(\varphi_l, \lambda_l) \right] q_{1,k}, \end{aligned}$$

according to the determined parameters 3–8 of  $x_k$ . Some of them depend on the map projection  $\mathbb{P}$ , the other are independent. This technique brings a refinement of the hybrid method presented in [4].

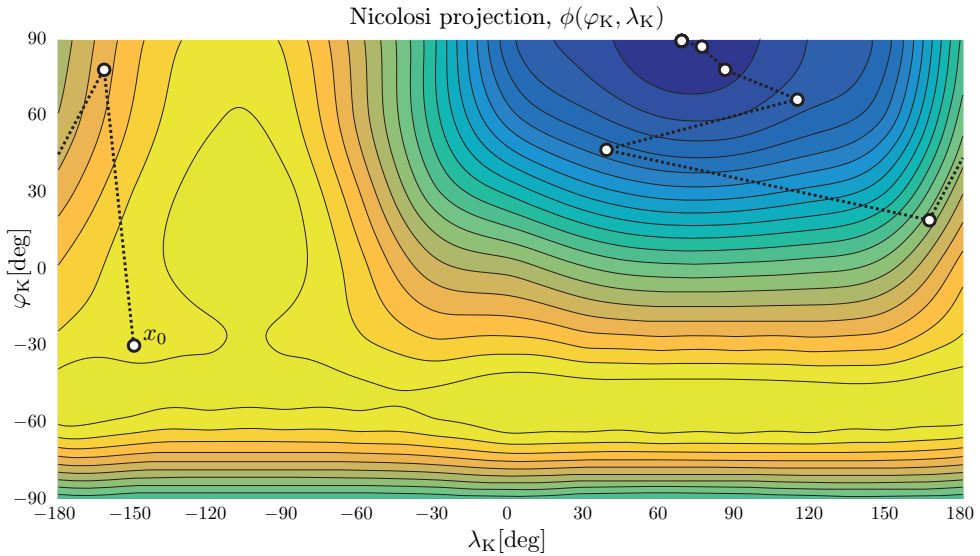


Figure 4.1. The iteration process illustrates the convergence of  $\phi(\varphi_K, \lambda_K)$  to the optimizer  $\hat{x} = [89.79^\circ, 70.07^\circ]$  for the Eastern Hemisphere of the analyzed map in the Nicolosi globular projection (see Sec. 6.2).

**4.1. Solving nonlinear least squares.** Suppose the minimized function is  $\phi(x) = \frac{1}{2}r^T(x)r(x)$ . The nonlinear least squares finds the optimizer  $\hat{x}$  associated with the projection  $\mathbb{P}_x$ . This task may be solved for the unlimited set of projections

$$\tilde{x} = \arg \min_{\forall \mathbb{P}_x} \phi(x).$$

For large residuals or ill-conditioned tasks, the hybrid methods combining the first-order (Gauss-Newton) and second-order (quasi-Newton) methods provide an efficient solution. The map projection analysis represents a “small problem”,  $n \leq 10$ ; the over-determined system leads to the singular Jacobian matrix  $J$ . While the early maps provide large residuals, the current maps bring small (almost zero) residuals. For zero-residual problems the quadratic rate of convergence occurs, otherwise the superlinear convergence is guaranteed. This approach has been studied in many papers, for example in [1], [11], [18], [20], [31], for sparse nonlinear least squares in [19]. The equation

$$\tau = \frac{\phi(x_k) - \phi(x_{k+1})}{\phi(x_k)}$$

indicates which actualization step will be taken. If  $\tau > \tau_{\min}$ ,  $B(x_{k+1})$  is determined from the Gauss-Newton method, if  $\tau < \tau_{\min}$  and  $y_k^T s_k > 0$ , the BFGS update is used:

$$(4.2) \quad B(x_{k+1}) = \begin{cases} J^T(x_{k+1})J(x_{k+1}), & \tau > \tau_{\min}, \\ B(x_k) + \frac{y_k y_k^T}{y_k^T s_k} - \frac{B(x_k) s_k s_k^T B^T(x_k)}{s_k^T B(x_k) s_k}, & \tau < \tau_{\min}, y_k^T s_k > 0, \end{cases}$$

where  $\tau_{\min} = 0.0001$ , and  $s_k = x_{k+1} - x_k$ ,  $y_k = \nabla \phi(x_{k+1}) - \nabla \phi(x_k)$ . Alternately, the structured methods combining the Gauss-Newton and variable-metric methods may be used; this approach has been studied in several papers, for example in [13], [29].

The optimal step has been found using both the trust-region (dog-leg method, iterative solution) and line search strategies. Comparing both strategies, the trust-region approach is more efficient (less iterations and failures) for the projection analysis; the hybrid method has a fast convergence rate. In general, 20 iterations are sufficient.

For the analyzed early map from Sec. 6.2, the fast convergence of  $\phi(\varphi_K, \lambda_K)$  is visualized in Fig. 4.1. The reconstructed graticules of the estimated Nicolosi globular projection (close to the normal aspect) for iterations 2–8 can be found in Fig. 4.2.

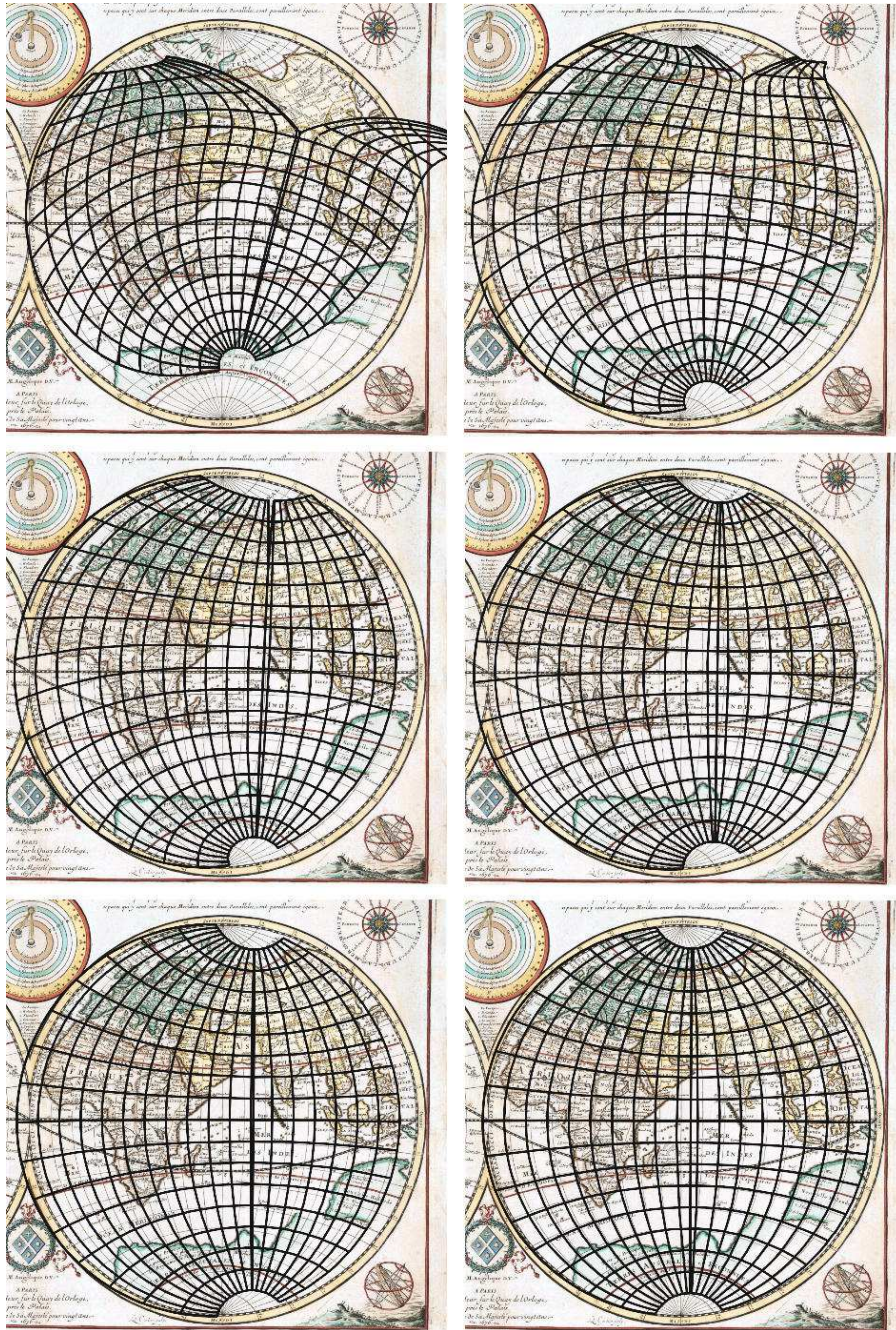


Figure 4.2. Analysis of the early map projection using the trust region approach, iterations 2–8. The graticules of the Nicolosi globular projection for the Eastern Hemisphere are reconstructed from the current values of  $x_k$ .

## 5. RE-PROJECTION OF THE MAP

When working with various maps it is necessary to unify their map projections, unless their projections are identical or very similar. This leads to the sequence of re-projections of the analyzed map from its “native” projection to the destination projection. Typically, a projection associated with the national coordinate systems is preferred (e.g. the transverse Mercator or Lambert azimuthal projections). For maps without any information about the map projection, the above-mentioned analysis needs to be undertaken.

The current strategy of re-projection, based on the application of different types of transformations, is not applicable to large territories. It has only limited utilization for maps of small territories and cannot correct the impact of distortions. Increasing the territory size, its shape becomes less similar in different projections. Fig. 5.1 illustrates that these discrepancies cannot be corrected without a knowledge of the map projection equations. Finding the inverse projection is a crucial step of map re-projection.

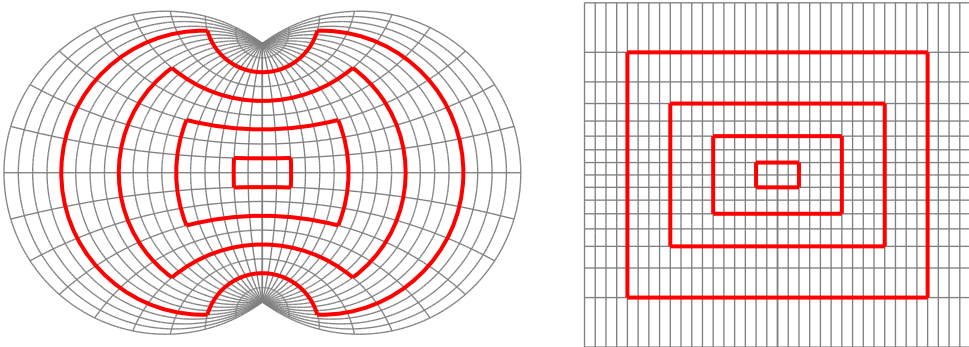


Figure 5.1. Different shapes of territories in the Nicolosi globular and Mercator projections; the Nicolosi globular projection is extended for the entire planisphere.

**5.1. Differential equations of inverse transformation.** The nonsingular projection  $\mathbb{P}$  between local coordinate systems  $[\varphi, \lambda] \in (-\frac{\pi}{2}, \frac{\pi}{2}) \times (-\pi, \pi)$  of the sphere  $\mathbb{S}^2$  and  $[X, Y] \in \mathbb{R}^2$  of the plane is given by

$$(5.1) \quad X = X(\varphi, \lambda), \quad Y = Y(\varphi, \lambda).$$

In accordance with Theorem 3.7, the inverse projection  $\mathbb{P}^{-1}$  exists such that

$$(5.2) \quad \varphi = \varphi(X, Y), \quad \lambda = \lambda(X, Y).$$

The differentials of coordinate functions are

$$(5.3) \quad \mathbb{P}: \begin{bmatrix} dX \\ dY \end{bmatrix} = \begin{bmatrix} \frac{\partial X}{\partial \varphi} & \frac{\partial X}{\partial \lambda} \\ \frac{\partial Y}{\partial \varphi} & \frac{\partial Y}{\partial \lambda} \end{bmatrix} \begin{bmatrix} d\varphi \\ d\lambda \end{bmatrix}, \quad \mathbb{P}^{-1}: \begin{bmatrix} d\varphi \\ d\lambda \end{bmatrix} = \begin{bmatrix} \frac{\partial \varphi}{\partial X} & \frac{\partial \varphi}{\partial Y} \\ \frac{\partial \lambda}{\partial X} & \frac{\partial \lambda}{\partial Y} \end{bmatrix} \begin{bmatrix} dX \\ dY \end{bmatrix}.$$

From the equation for  $\mathbb{P}$  in (5.3) the vector of the differentials of the spherical coordinates can be found using the inverse matrix

$$\begin{bmatrix} d\varphi \\ d\lambda \end{bmatrix} = \frac{1}{D} \begin{bmatrix} \frac{\partial Y}{\partial \lambda} & -\frac{\partial X}{\partial \lambda} \\ -\frac{\partial Y}{\partial \varphi} & \frac{\partial X}{\partial \varphi} \end{bmatrix} \begin{bmatrix} dX \\ dY \end{bmatrix},$$

and, after a comparison,

$$\frac{\partial Y}{\partial \lambda} = D \frac{\partial \varphi}{\partial X}, \quad \frac{\partial X}{\partial \lambda} = -D \frac{\partial \varphi}{\partial Y}, \quad \frac{\partial Y}{\partial \varphi} = -D \frac{\partial \lambda}{\partial X}, \quad \frac{\partial X}{\partial \varphi} = D \frac{\partial \lambda}{\partial Y},$$

where

$$(5.4) \quad D = \frac{\partial X}{\partial \varphi} \frac{\partial Y}{\partial \lambda} - \frac{\partial X}{\partial \lambda} \frac{\partial Y}{\partial \varphi}, \quad \frac{1}{D} = \frac{\partial \varphi}{\partial X} \frac{\partial \lambda}{\partial Y} - \frac{\partial \varphi}{\partial Y} \frac{\partial \lambda}{\partial X}.$$

Matrix  $\mathbb{P}$  columns are the tangent vectors of curves in the plane with the squares

$$(5.5) \quad \left( \frac{\partial \lambda}{\partial X} \right)^2 + \left( \frac{\partial \lambda}{\partial Y} \right)^2 = D^2 \left[ \left( \frac{\partial X}{\partial \varphi} \right)^2 + \left( \frac{\partial Y}{\partial \varphi} \right)^2 \right],$$

$$(5.6) \quad \left( \frac{\partial \varphi}{\partial X} \right)^2 + \left( \frac{\partial \varphi}{\partial Y} \right)^2 = D^2 \left[ \left( \frac{\partial X}{\partial \lambda} \right)^2 + \left( \frac{\partial Y}{\partial \lambda} \right)^2 \right],$$

their dot product is

$$(5.7) \quad \frac{\partial X}{\partial \varphi} \frac{\partial X}{\partial \lambda} + \frac{\partial Y}{\partial \varphi} \frac{\partial Y}{\partial \lambda} = -D^2 \left( \frac{\partial \varphi}{\partial X} \frac{\partial \varphi}{\partial Y} + \frac{\partial \lambda}{\partial X} \frac{\partial \lambda}{\partial Y} \right).$$

**Definition 5.1.** The quadratic differential form

$$ds^2 = E d\varphi^2 + 2F d\varphi d\lambda + G d\lambda^2$$

is called the first fundamental form of the plane, where the factors  $E, F, G$  are the left-hand sides of (5.5), (5.6), (5.7).

**Remark 5.2.** The first fundamental form of the sphere  $F(\varphi, \lambda) = [R \cos \varphi \cos \lambda, R \cos \varphi \sin \lambda, R \sin \varphi]$  is the quadratic surface  $ds^2 = R^2 d\varphi^2 + R^2 \cos^2 \varphi d\lambda^2$ . From their fraction the local linear scale in the meridian direction is

$$h = \frac{\sqrt{E}}{R},$$

the local linear scale in the parallel direction is

$$k = \frac{G}{R \cos \varphi},$$

and the aerial scale is

$$(5.8) \quad P = \frac{D}{R^2 \cos \varphi}.$$

Substituting this into (5.5) and (5.6) leads to

$$(5.9) \quad \left(\frac{\partial \varphi}{\partial X}\right)^2 + \left(\frac{\partial \varphi}{\partial Y}\right)^2 = \left(\frac{k}{RP}\right)^2,$$

$$(5.10) \quad \left(\frac{\partial \lambda}{\partial X}\right)^2 + \left(\frac{\partial \lambda}{\partial Y}\right)^2 = \left(\frac{h}{RP \cos \varphi}\right)^2.$$

**Definition 5.3.** The nonlinear partial differential equations (5.9), (5.10) for functions (5.2) are the equations of the inverse projection.

For  $\partial \varphi / \partial X$ ,  $\partial \varphi / \partial \lambda$  determined from Eq. (5.9) the problem may be simplified. Using the reciprocal form of (5.8)

$$\frac{1}{PR^2 \cos \varphi} = \frac{1}{D} = \frac{\partial \varphi}{\partial X} \frac{\partial \lambda}{\partial Y} - \frac{\partial \varphi}{\partial Y} \frac{\partial \lambda}{\partial X},$$

the linear partial differential equation of the inverse function is

$$(5.11) \quad R^2 P \cos \varphi \left( \frac{\partial \varphi}{\partial X} \frac{\partial \lambda}{\partial Y} - \frac{\partial \varphi}{\partial Y} \frac{\partial \lambda}{\partial X} \right) = 1.$$

Alternatively, the area of the infinitesimal quadrangle is given by

$$dA = R^2 \cos \varphi d\varphi d\lambda.$$

For the longitude extent of  $\Delta \lambda = \lambda_2 - \lambda_1 = 1$  we have

$$\frac{d\varphi}{dA} = \frac{1}{R^2 \cos \varphi}$$

and

$$\frac{1}{P} = \frac{\partial A}{\partial \varphi} \frac{\partial \varphi}{\partial X} \frac{\partial \lambda}{\partial Y} - \frac{\partial A}{\partial \varphi} \frac{\partial \varphi}{\partial Y} \frac{\partial \lambda}{\partial X} = \frac{\partial A}{\partial X} \frac{\partial \lambda}{\partial Y} - \frac{\partial A}{\partial Y} \frac{\partial \lambda}{\partial X};$$

this leads to the linear partial differential equation of the inverse function

$$(5.12) \quad P \left( \frac{\partial A}{\partial X} \frac{\partial \lambda}{\partial Y} - \frac{\partial A}{\partial Y} \frac{\partial \lambda}{\partial X} \right) = 1.$$

**5.2. Straightforward inverse.** For most map projections the solution of partial differential equations is nontrivial, so the straightforward inverse of the coordinate functions is more appropriate. Unfortunately, for transcendent equations only the numerical solution is available (e.g. Newton-Raphson method). Here are examples of commonly used families of map projections and their inverses. For the cylindrical projection

$$(X, Y) = (F(\lambda), cG(\varphi)), \quad c \in [0, 1],$$

its inverse has the simple form of

$$(\varphi, \lambda) = \left( G^{-1} \left( \frac{Y}{c} \right), F^{-1}(X) \right).$$

For the azimuthal projection

$$(5.13) \quad (X, Y) = (\varrho \sin \lambda, \varrho \cos \lambda),$$

where  $\varrho = f(\psi)$ ,  $\psi = \frac{1}{2}\pi - \varphi$ , the inverse is

$$(5.14) \quad \lambda = \arctan \frac{X}{Y}, \quad \psi = f^{-1}(\varrho), \quad \varrho = \sqrt{X^2 + Y^2}.$$

For the conic projection

$$(5.15) \quad (X, Y) = (\varrho \sin \delta, \varrho_0 - \varrho \cos \delta),$$

where  $\varrho = f(\varphi)$ ,  $\delta = c\lambda$ , we have

$$(5.16) \quad \delta = \arctan \frac{X}{\Delta Y}, \quad \varrho = \sqrt{X^2 + \Delta Y^2},$$

and  $\Delta Y = \varrho_0 - Y$ . Its inverse is written as

$$(\varphi, \lambda) = \left( f^{-1}(\varrho), \frac{\delta}{c} \right).$$

The pseudocylindrical projection

$$(X, Y) = (F(\varphi, \lambda), G(\varphi))$$

has a simple form of inverse

$$(\varphi, \lambda) = (G^{-1}(Y), F^{-1}(\varphi, X)).$$

For its equal area variant

$$(X, Y) = (F(\varphi, \lambda, \theta), G(\varphi, \theta)), \quad f(\varphi, \theta) = 0,$$

the arbitrary condition is rewritten to  $\varphi = f^{-1}(\theta)$  and  $\theta$  is determined using the Newton-Raphson method

$$\theta_{i+1} = \theta_i - \frac{h(\theta)}{h'(\theta)}, \quad h(\theta) = G(f^{-1}(\theta), \theta) - Y = 0.$$

Finally,

$$(\varphi, \lambda) = (g(\theta), F^{-1}(\varphi, X)).$$

The general form of the pseudoconic projection is analogous to (5.15), where  $\varrho = f(\varphi)$ ,  $\delta = g(\varphi, \lambda)$ . The polar coordinates  $\varrho$ ,  $\delta$  are evaluated from (5.16), the inverse form is

$$(\varphi, \lambda) = (f^{-1}(\varrho), g^{-1}(\varphi, \delta)).$$

The general form of the pseudoazimuthal projection is analogous to (5.13), where  $\varrho = f(\psi)$ ,  $\delta = g(\varphi, \lambda)$ . The polar coordinates  $\varrho$ ,  $\delta$  can be evaluated from (5.14), the inverse projection is

$$(\varphi, \lambda) = \left( \frac{\pi}{2} - f^{-1}(\varrho), g^{-1}(\varphi, \delta) \right).$$

For a polyconic projection

$$(X, Y) = (\varrho \sin \delta, S + \varrho(1 - \cos \delta)),$$

where  $\varrho = f(\varphi)$ ,  $\delta = g(\varphi, \lambda)$ ,  $S = h(\varphi)$ , using the substitution  $\Delta Y = S + \varrho - Y$ , we obtain

$$\varrho^2 = X^2 + \Delta Y^2.$$

The latitude  $\varphi$  may be determined from

$$\varphi_{i+1} = \varphi_i - \frac{H(\varphi)}{H'(\varphi)}, \quad H(\varphi) = X^2 + \Delta Y^2 - \varrho^2 = X^2 + (S + \varrho - Y)^2 - \varrho^2,$$

where  $S$ ,  $\varrho$  are determined from (5.16) and

$$\lambda = g^{-1}(\varphi, \delta).$$

For some families of projections, where  $X = F(\varphi, \lambda)$ ,  $Y = G(\varphi, \lambda)$ , typically globular or nonclassified projections, there is no general scheme to find their inverse; each projection is processed individually.

**5.3. Re-projection of the map.** The analyzed map projection  $\mathbb{P}_1$  is given by the equations

$$(5.17) \quad (X, Y) = (F_1(\varphi, \lambda), G_1(\varphi, \lambda)),$$

its inverse  $\mathbb{P}_1^{-1}$  can be found in the form:

$$(5.18) \quad (\varphi, \lambda) = (F_1^{-1}(X, Y), G_1^{-1}(X, Y)).$$

During the re-projection, the map in the source projection  $\mathbb{P}_1$  is transformed to the unified (e.g. destination) projection  $\mathbb{P}_2$ . This procedure can be written as

$$(5.19) \quad \begin{aligned} (x, y) &= (F_2(\varphi, \lambda), G_2(\varphi, \lambda)) \\ &= (F_2(F_1^{-1}(X, Y), G_1^{-1}(X, Y)), G_2(F_1^{-1}(X, Y), G_1^{-1}(X, Y))). \end{aligned}$$

For the oblique aspect of the projection it consists of three substeps:  $(X, Y) \rightarrow (\varphi', \lambda') \rightarrow (\varphi, \lambda) \rightarrow (x, y)$ . The inverse of  $\mathbb{P}_1$  can be found using the above-mentioned formulas.

## 6. EXPERIMENTS AND RESULTS

In this section the above-mentioned principles will be illustrated on the early map analysis and finding the inverse projections. While the differential equations for the inverse transformation are solved for the stereographic projection (relatively simple form of coordinate functions), the straightforward approach is used for the Nicolosi projection. Both projections (stereographic projection in the transverse aspect) frequently used for early maps have an analogous shape of the graticule. For the analyzed world map in the planisphere created in the Nicolosi projection, its new equations extended for the entire planisphere as well as its inverse will be derived. Subsequently, the early map will be re-projected to the Mercator projection used in Open Street Maps.

**6.1. Inverse of the stereographic projection.** Stereographic projection has been used in two hemispheres for world maps since the time of Ancient Greece.

**Definition 6.1.** The stereographic projection is a central projection of the sphere  $\mathbb{S}^2$  from a viewing point  $Q$  to the tangent (or parallel) plane  $\sigma$  in the point opposite to  $Q$ .

**Theorem 6.2.** *The coordinate functions of the stereographic projection of the sphere  $\mathbb{S}^2$  given by the radius  $R$  from its South Pole to a plane tangent in the North Pole are*

$$(6.1) \quad (X, Y) = (\varrho \sin \lambda, \varrho \cos \lambda), \quad \varrho = 2R \tan\left(\frac{\pi}{4} - \frac{\varphi}{2}\right).$$

It represents a conformal projection, where

$$h = k = \frac{1}{\cos^2(\pi/4 - \varphi/2)}, \quad P = h^2 = \frac{1}{\cos^4(\pi/4 - \varphi/2)}.$$

Substituting this into (5.9) and (5.10), the differential equations of the inverse stereographic projection are

$$(6.2) \quad \left(\frac{\partial\varphi}{\partial X}\right)^2 + \left(\frac{\partial\varphi}{\partial Y}\right)^2 = \left(\frac{1 + \sin\varphi}{2R}\right)^2,$$

$$(6.3) \quad \left(\frac{\partial\lambda}{\partial X}\right)^2 + \left(\frac{\partial\lambda}{\partial Y}\right)^2 = \frac{1}{\varrho^2}.$$

On (6.3) the right-hand side is a constant

$$\left(\frac{\partial\lambda}{\partial X}\right)^2 + \left(\frac{\partial\lambda}{\partial Y}\right)^2 = c^2.$$

After the substitution  $\partial\lambda/\partial x = a$ , we obtain

$$\frac{\partial\lambda}{\partial Y} = \sqrt{c^2 - a^2}$$

and

$$\lambda = aX + \sqrt{c^2 - a^2}Y + b,$$

where  $b \in \mathbb{R}$  is a constant. The single-parameter system of planes with a normal vector  $(a, \sqrt{c^2 - a^2}, -1)$ , which forms a constant angle with the  $Z$  axis

$$\sin\varphi = \frac{1}{\sqrt{c^2 + 1}}(a, \sqrt{c^2 - a^2}, -1) \cdot (0, 0, 1) = \frac{-1}{c^2 + 1},$$

represents a conical surface,  $\cos\varphi = c/\sqrt{c^2 + 1}$  and  $1/\tan\varphi = c$ . Rotating the line  $\lambda - b = cX$  leads to

$$(\lambda - b)^2 = c^2(X^2 + Y^2),$$

where  $b = R$ , its parametric equations are

$$(X, Y, Z) = \left( u \frac{\sin \lambda}{\tan \varphi}, u \frac{\cos \lambda}{\tan \varphi}, R + \frac{u}{\tan \varphi} \right),$$

where  $u > 0$ . Hence, the inverse equation for  $\lambda$  is

$$\lambda = \arctan \frac{X}{Y}.$$

For the second coordinate function (6.2), using the substitution  $t = -aX - bY$ , we obtain

$$\frac{\partial \varphi}{\partial X} = \frac{\partial \varphi}{\partial t} \frac{\partial t}{\partial X} = -a \frac{\partial \varphi}{\partial t}, \quad \frac{\partial \varphi}{\partial Y} = \frac{\partial \varphi}{\partial t} \frac{\partial t}{\partial Y} = -b \frac{\partial \varphi}{\partial t}.$$

The back substitution brings the differential equation

$$\left( \frac{\partial \varphi}{\partial t} \right)^2 (a^2 + b^2) = \frac{(1 + \sin \varphi)^2}{4R^2}$$

with the solution

$$\int \frac{d\varphi}{1 + \sin \varphi} = \frac{1}{2R\sqrt{a^2 + b^2}} \int dt + c,$$

$$\tan\left(\frac{\pi}{4} - \frac{\varphi}{2}\right) = -\frac{ax + by}{2R\sqrt{a^2 + b^2}} + c,$$

where the initial condition is  $\varphi = \pi/2 \Rightarrow c = 0$ . Because

$$\frac{1}{\sqrt{a^2 + b^2}}(a, b) = \frac{1}{\varrho}(x, y)$$

is the normalized gradient of contours, we have

$$\tan\left(\frac{\pi}{4} - \frac{\varphi}{2}\right) = -\frac{x^2 + y^2}{2R\sqrt{x^2 + y^2}} = -\frac{\varrho}{2R}$$

and the inverse equation for  $\varphi$  is

$$\varphi = \frac{\pi}{2} - 2 \arctan \frac{\varrho}{2R}.$$

**Theorem 6.3.** *The inverse of the stereographic projection given by (6.1) is represented by the equations*

$$\varphi = \frac{\pi}{2} - 2 \arctan \frac{\varrho}{2R}, \quad \lambda = \arcsin \frac{X}{\varrho}, \quad \lambda = \arccos \frac{Y}{\varrho}, \quad \varrho^2 = X^2 + Y^2.$$

**6.2. Analysis of the early map projection.** The analyzed map “*Planisphere, ou Carte Generale du Monde*” assigned to the French geographer Duval (1619–1683), see Fig. 6.1, was created in 1676. His uncle, the famous cartographer Nicolas Sanson (1600–1667), is well-known as the inventor of several map projections (Sanson’s pseudocylindrical). This world map in two hemispheres uses the Nicolosi projection in the normal aspect with the shifted central meridian. Due to graphical inaccuracies of the map frame, the graticule, as well as the lack of solid geometric and geodesic bases, some discrepancies of the determined parameters are expected. The oblique aspect of the map is expected to be close to the normal one. The analyzed map is slightly rotated at the angle  $\alpha \doteq 0.5^\circ$ .

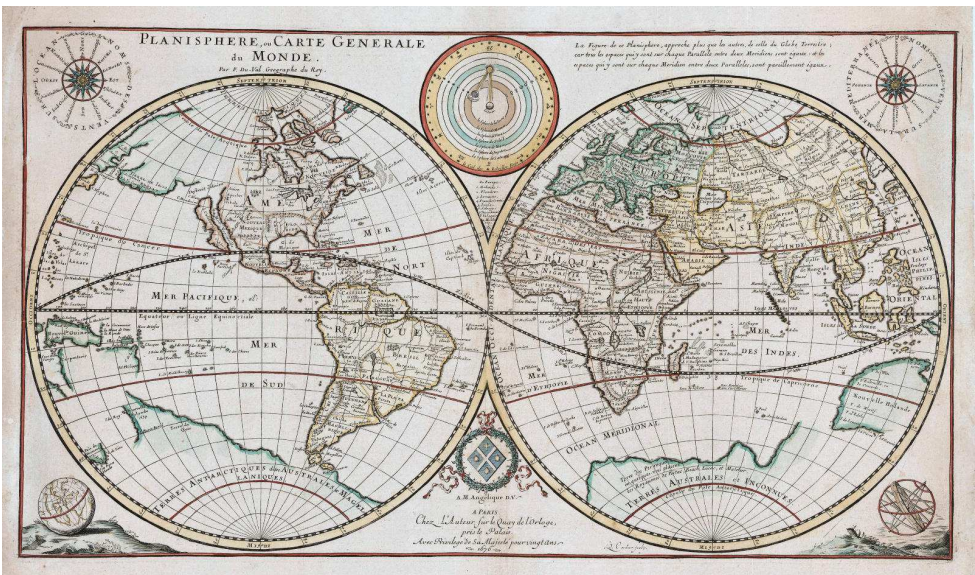


Figure 6.1. The analyzed map “*Planisphere, ou Carte Generale du Monde*” in the Nicolosi globular projection.

The Nicolosi globular projection discovered by the Persian geographer Abū Rayḥān Muhammad ibn Ahmad al-Bīrūnī (973–1048) was reinvented by the Italian geographer Giovanni Battista Nicolosi (1610–1676). Since the hemisphere was represented by a circle, the meridian/parallel are the circular arcs centered at the central meridian/equator, the projection was simple to construct and easy to use. The hemisphere projects as the circle centered at  $O$  with the radius  $R = 1$ ; see Fig. 6.2. The image of the prime meridian (involving the North and South Poles) is the circle diameter, the perpendicular diameter is represented by the equator. The remaining meridians and parallels are circular arcs centered at  $AB$ ,  $CD$ , where the series of intersections at  $AB$  and  $CD$  are equidistant.

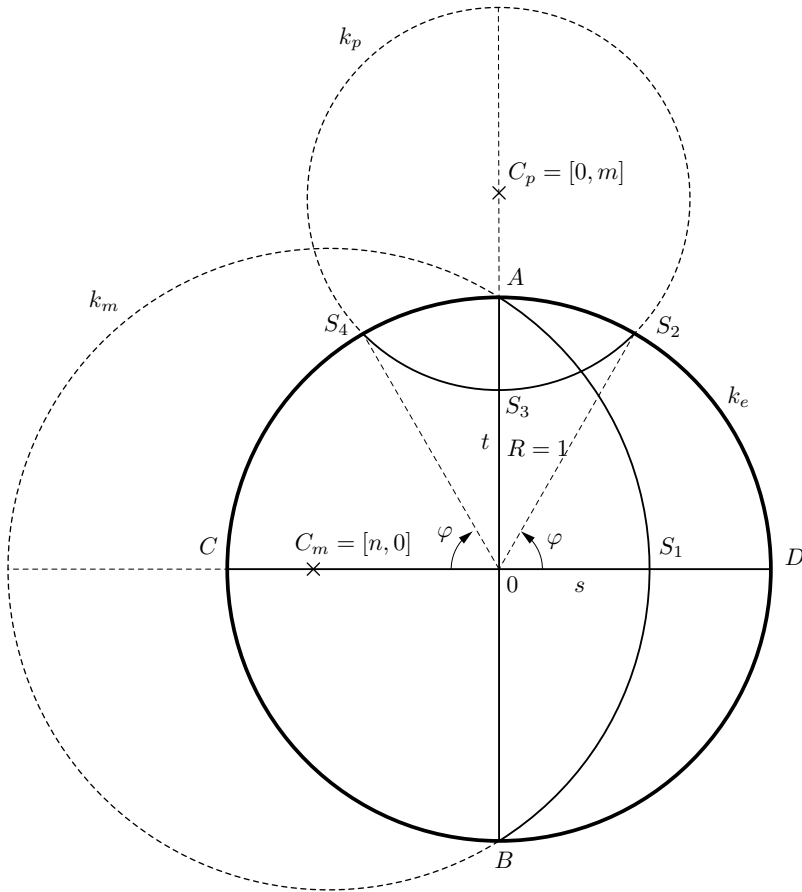


Figure 6.2. Geometric description of the Nicolosi globular projection.

**Images of parallels.** Let us denote by  $t \in \langle 0, 1 \rangle$  the distance of the lowest point of the arc from the center  $O$ . Hence, the image of the parallel of latitude  $\varphi$  passes through points  $S_3 = [0, t]$  and  $S_2 = [\cos \varphi, \sin \varphi]$ . The arc center  $C_p = [0, m]$  is the intersection of  $y = AB$  and the axis of  $S_3, S_2$ , where

$$m = \frac{1 - t^2}{2(\sin \varphi - t)}.$$

The relationship between  $t$  and  $\varphi$  is determined from the direct proportionality  $\varphi : \frac{\pi}{2} = t : 1$ . The arc radius is

$$r = m - t.$$

**Images of meridians.** They pass through the poles  $A, B$ , the next point  $S_1 = [s, 0]$  lies on  $x = CD$ , the distance from  $O$  is denoted as  $s \in \langle 0, 1 \rangle$ . The arc center

$C_m = [n, 0]$  is the intersection of  $x$  and the axis  $AS_1$ , where

$$(6.4) \quad n = \frac{s^2 - 1}{2s}.$$

The relationship between  $s$  and  $\lambda$  is determined from the direct proportionality  $\lambda : \frac{\pi}{2} = s : 1$  and the arc radius is

$$r' = s + |n| = \frac{1 + s^2}{2s}.$$

To find the intersection of the meridian and parallel arcs, solve the system of equations

$$(6.5) \quad (x - n)^2 + y^2 = 1 + n^2, \quad x^2 + (y - m)^2 = (m - t)^2,$$

where  $x$  can be found from the quadratic equation

$$(4m^2 + 4n^2)x^2 + (4n + 8mnt - 4nt^2 + 8mn^2)x + m^2(1 + 4m^2t^2 + 4mt - 2t^2 - 4mt^3 - 4m^2) = 0.$$

The second coordinate  $y$  is evaluated using the back substitution to (6.5). Considering the projection symmetry to  $AB$ ,  $CD$ , then  $x, y$  take the signs of  $\lambda, \varphi$ . For the sphere with the radius  $R$ , the Nicolosi projection equations are written as

$$X = Rx, \quad Y = Ry.$$

It is interesting that the derived formulas generalize the Nicolosi globular projection for the entire planisphere, see Fig. 5.1. With regard to the projection equations, a numerical differentiation for the Jacobian matrix entries is recommended.

**Results of the analysis.** For the analysis, 32 identical points in the Western Hemisphere and 37 points in the Eastern Hemisphere, the intersections of meridians and parallels, where  $\Delta\varphi = \Delta\lambda = 30^\circ$ , were collected. The iteration process for the Eastern Hemisphere can be found in Figs. 4.1, 4.2, the results of both hemispheres are summarized in Tab. 1. Both the hemispheres achieved consistent results, the Nicolosi globular projection close to the normal aspect and the azimuthal equidistant projection close to the transverse aspect are recommended as the best two candidates. The central meridian is shifted by  $\lambda'_0 = -110^\circ$  for the Western and  $\lambda'_0 = 70^\circ$  for the Eastern Hemispheres. In the normal aspect,  $\lambda_K$  and  $\lambda_0$  are linearly dependent; the central meridian shift  $\lambda_0$  may be compensated by changing  $\lambda_K$ . For the estimated

#	Projection	Family	$\phi$	$R'$	$\varphi_K$	$\lambda_K$	$\varphi'_1$	$\varphi'_2$	$\lambda'_0$	$S$	$\alpha$	$\kappa$
Eastern Hemisphere												
1	Nicolosi	Globular	$3.82 \cdot 10^2$	473.57	89.79	70.07	x	x	0.00	159120098	-0.23	0.00
2	Equidistant	Azimuthal	$5.22 \cdot 10^3$	473.36	-0.23	69.96	x	x	0.00	159191568	-0.23	0.00
3	Far side	Azimuthal	$5.28 \cdot 10^3$	469.43	-0.21	69.89	x	x	0.00	160521989	-0.23	2.75
4	La Hire	Azimuthal	$5.34 \cdot 10^3$	466.72	-0.22	69.92	x	x	0.00	161456124	-0.23	0.00
5	Equidistant	Conic	$5.83 \cdot 10^3$	473.34	0.09	69.94	85.00	13.78	0.00	159195885	-0.23	0.00
Western Hemisphere												
1	Nicolosi	Globular	$3.02 \cdot 10^2$	473.18	89.96	-110.30	x	x	0.00	159259930	-0.43	0.00
2	Equidistant	Azimuthal	$4.34 \cdot 10^3$	472.79	0.10	-111.12	x	x	0.00	159381611	-0.43	0.00
3	Far side	Azimuthal	$4.35 \cdot 10^3$	469.90	0.13	-111.16	x	x	0.00	160362105	-0.44	2.78
4	La Hire	Azimuthal	$4.44 \cdot 10^3$	466.16	0.10	-111.07	x	x	0.00	161650167	-0.44	0.00
5	Equidistant	Conic	$4.83 \cdot 10^3$	472.78	0.49	-111.18	85.00	-57.95	0.00	159386846	-0.44	0.00

Table 1. The analyzed map: 5 best-fit projections sorted according to the objective function  $\phi$  values for the Eastern and Western Hemispheres. The symbol x indicates that a projection does not use true parallels.

map scale  $S \doteq 1 : 160000000$  (refers to  $R = 6380$  km, and  $i_r = 300$  DPI), the residuals are below the graphical accuracy of the analyzed map and provide a good fit. While the Western Hemisphere is rotated by the angle  $\alpha = -0.43^\circ$ , the Eastern Hemisphere is rotated by  $\alpha = -0.23^\circ$ . The early map graticule reconstructed from the vector  $x$  of the estimated parameters can be found in Fig. 6.3.

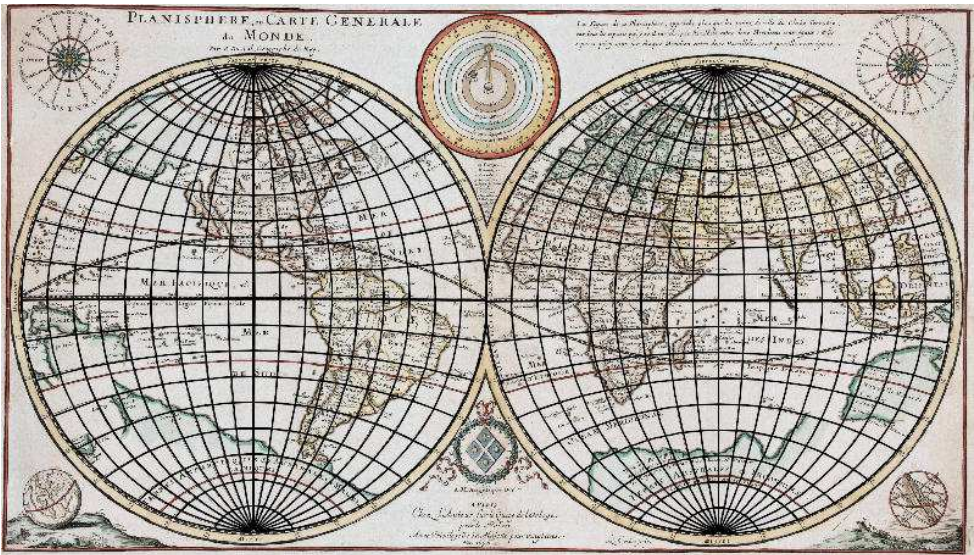


Figure 6.3. The reconstructed graticule of the analyzed map in the Nicolosi globular projection, Eastern and Western Hemispheres.

**6.3. Inverse of the projection.** For the re-projection of the analyzed map to the sphere, the inverse form of the Nicolosi globular projection needs to be found. Due to the complexity of the coordinate functions  $F, G$ , the straightforward inverse will be used. Initially, the reduced coordinates on the unit sphere  $\mathbb{S}^2$  are

$$x = \frac{X}{R}, \quad y = \frac{Y}{R}.$$

From (6.4) and (6.5) we get

$$1 - 2sn - s^2 = 0, \quad x^2 + y^2 + 2nx = 1,$$

where  $s$  can be found from the quadratic equation

$$xs^2 + (1 - x^2 - y^2)s - x = 0,$$

and the longitude  $\lambda = \frac{1}{2}\pi s$  takes the sign of  $X$ . From (6.5) the transcendental equation for  $\varphi$

$$\begin{aligned} H(\varphi)^2 &= x^2 + y^2 + 2m(t - y) - t^2 = 0, \\ &= (x^2 + y^2)(\pi \sin \varphi - 2\varphi)\pi + 4\varphi^2(Y - \sin \varphi) + 2\pi\varphi - \pi^2 y \end{aligned}$$

is solved using the Newton-Raphson method

$$H'_\varphi = (x^2 + y^2)(\pi \cos \varphi - 2)\pi + 8\varphi(y - \sin \varphi) - 4\varphi^2 \cos \varphi + 2\pi.$$

Hence, the pixel coordinates  $(X_i, Y_i)$  of the raster in projection  $\mathbb{P}_1$  are transformed to the unit sphere  $\mathbb{S}^2$ :  $(\varphi_i, \lambda_i) = (F_1^{-1}(X_i, Y_i), G_1^{-1}(X_i, Y_i))$ .

**6.4. Re-projection of the map.** The final step is represented by the re-projection of the analyzed map from the sphere  $\mathbb{S}^2$  to the destination projection  $\mathbb{P}_2$ . Due to the fact that the Open Street Maps have been used as the reference maps,  $\mathbb{P}_2$  refers to the Web Mercator (EPSG 3857) given by the coordinate functions

$$(x, y) = \left( R\lambda \cos \varphi_1, R \ln \left[ \tan \left( \frac{\varphi}{2} + \frac{\pi}{4} \right) \right] \right),$$

where  $\varphi_1 = 50^\circ$ . Any pixel  $(\varphi_i, \lambda_i)$  on  $\mathbb{S}^2$  is re-projected to  $\mathbb{P}_2$  so that:  $(x_i, y_i) = (F_2(\varphi_i, \lambda_i), G_2(\varphi_i, \lambda_i))$ . Because of singularities, all pixels of the latitude  $|\varphi_i| > 80^\circ$  are omitted from the transformation. The re-projected map in the Mercator projection in Fig. 6.4 illustrates the lack of solid geodesic bases, the shapes of continents are stretched in the east-west direction. This typical issue due to the uncertainty in

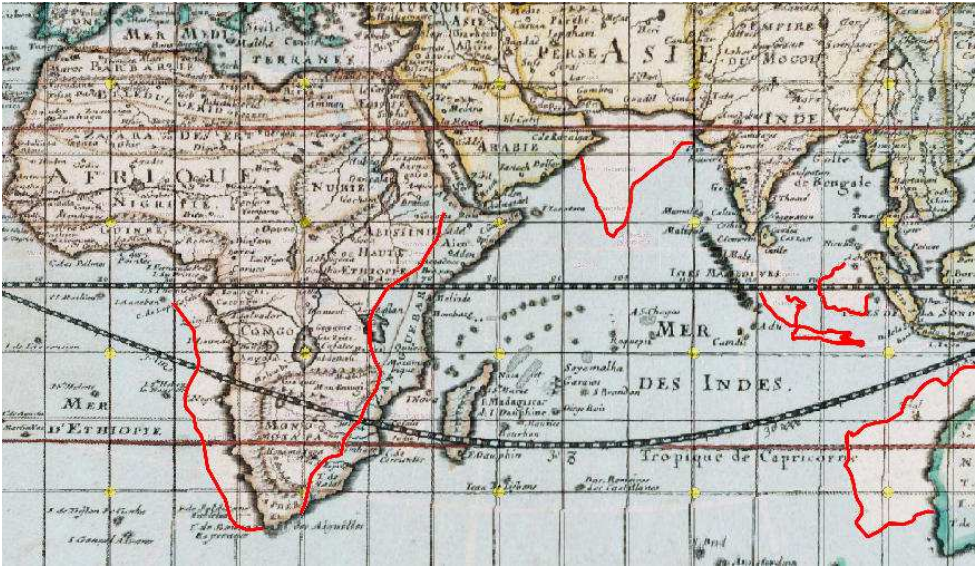


Figure 6.4. A comparison of the analyzed map in the Nicolosi globular projection re-projected to the Mercator projection and the outlines of the continents in Open Street Maps; the continents are stretched in the east-west direction.

longitude was corrected with the invention of the precise marine chronometer (John Harrison, 1761).

**6.5. Software detectproj.** All proposed detection techniques and re-projection methods have been implemented in the new `detectproj` software. Currently, more than 100 map projections are supported, several inverse projection inverses are newly derived. The source code, written in Java and distributed under GNU/GPL2 license is available free of charge at

<https://sourceforge.net/projects/detectproj/>.

The software allows you to perform real-time analysis, two detection methods and three optimization techniques are supported. Because of user friendliness, all computations run in a separate thread. The determined parameters of the map projection can be visualized and used for the graticule reconstruction. As the background layer, the Mercator projection, to which the analyzed map may be re-projected, is used.

## 7. CONCLUSION

This article presented a new approach for automated map projection analysis, its inverse and re-projection. The above-mentioned methods are general, they can be applied to any map. An important role is played by the size of the analyzed territory, its location and shape. For the geographic extent  $\Delta\varphi = \Delta\lambda < 3^\circ$  it is almost impossible to determine the projection clearly; there are multiple candidates. The detection problem leads to unconstrained optimization solved using the nonlinear least squares. For reliable results, 10 identical points located over the entire map with a positional accuracy of better than 3 mm are required [4].

For the map projection inverse, the partial differential equations are derived. Since finding the closed-form solution is quite difficult the straightforward inverse of their coordinate functions is more suitable. These formulas may be used for the re-projection of the analyzed map to the destination coordinate system of current digital maps. Both approaches are illustrated for finding the inverse form of the Nicolosi globular and stereographic projections.

### References

- [1] *M. Al-Baali, R. Fletcher*: Variational methods for non-linear least-squares. *J. Oper. Res. Soc.* *36* (1985), 405–421. zbl doi
- [2] *Á. Barancsuk*: A semi-automatic approach for determining the projection of small scale maps based on the shape of graticule lines. *Progress in Cartography. EuroCarto 2015* (G. Gartner, M. Jobst, H. Huang, eds.). Springer, Cham, 2016, pp. 267–288. doi
- [3] *T. Bayer*: Estimation of an unknown cartographic projection and its parameters from the map. *GeoInformatica 18* (2014), 621–669. doi
- [4] *T. Bayer*: Advanced methods for the estimation of an unknown projection from a map. *GeoInformatica 20* (2016), 241–284. doi
- [5] *T. Bayer*: Detectproj—software for the projection analysis. Available at <http://sourceforge.net/projects/detectproj/> (2017).
- [6] *T. Bayer*: Plotting the map projection graticule involving discontinuities based on combined sampling. *Geoinformatics FCE CTU 17* (2018), 31–64. doi
- [7] *I. O. Bildirici*: Numerical inverse transformation for map projections. *Computers & Geosciences 29* (2003), 1003–1011. doi
- [8] *I. O. Bildirici*: An iterative approach for inverse transformation of map projections. *Cartography and Geographic Information Science 44* (2017), 463–471. doi
- [9] *G. I. Evenden*: *libproj4*: A comprehensive library of cartographic projection functions. Falmouth, Massachusetts, 2005.
- [10] *W. Flacke, B. Kraus*: *Working with Projections and Datum Transformations in ArcGIS: Theory and Practical Examples*. Points Verlag, Norden, 2005.
- [11] *R. Fletcher, C. Xu*: Hybrid methods for nonlinear least squares. *IMA J. Numer. Anal.* *7* (1987), 371–389. zbl MR doi
- [12] *E. Harrison, A. Mahdavi-Amiri, F. Samavati*: Optimization of inverse Snyder polyhedral projection. *Cyberworlds (CW), 2011 International Conference on Cyberworlds. IEEE*, 2011, pp. 136–143. doi

- [13] *J. Huschens*: On the use of product structure in secant methods for nonlinear least squares problems. *SIAM J. Optim.* *4* (1994), 108–129. [zbl](#) [MR](#) [doi](#)
- [14] *C. Ipbüker*: Inverse transformation for several pseudo-cylindrical map projections using Jacobian matrix. *International Conference on Computational Science and Its Applications* (O. Gervasi et al., eds.). Springer, Berlin, 2009, pp. 553–564. [doi](#)
- [15] *C. Ipbüker, I. Bildirici*: A general algorithm for the inverse transformation of map projections using jacobian matrices. *Proceedings of the Third International Symposium Mathematical & Computational Applications 2002*. Konya, Turkey, 2002, pp. 175–182.
- [16] *B. Jenny*: *Map Analyst*. Available at <http://mapanalyst.org>, 2011.
- [17] *M. Lapaine*: Mollweide map projection. *KoG* *15* (2011), 7–16. [zbl](#) [MR](#)
- [18] *L. Lukšan*: Computational experience with known variable metric updates. *J. Optimization Theory Appl.* *83* (1994), 27–47. [zbl](#) [MR](#) [doi](#)
- [19] *L. Lukšan*: Hybrid methods for large sparse nonlinear least squares. *J. Optimization Theory Appl.* *89* (1996), 575–595. [zbl](#) [MR](#) [doi](#)
- [20] *L. Lukšan, E. Spedicato*: Variable metric methods for unconstrained optimization and nonlinear least squares. *J. Comput. Appl. Math.* *124* (2000), 61–95. [zbl](#) [MR](#) [doi](#)
- [21] *D. A. Ratner*: An implementation of the Robinson map projection based on cubic splines. *Cartography and Geographic Information Systems* *18* (1991), 104–108. [doi](#)
- [22] *B. Šavrič, B. Jenny*: A new pseudocylindrical equal-area projection for adaptive composite map projections. *International Journal of Geographical Information Science* *28* (2014), 2373–2389. [doi](#)
- [23] *W. M. Smart, R. M. Green*: *Textbook on Spherical Astronomy*. Cambridge University Press, Cambridge, 1977. [doi](#)
- [24] *J. P. Snyder*: *Map Projections Used by the US Geological Survey*. Technical report, US Government Printing Office, Washington, 1982.
- [25] *J. P. Snyder*: *Map projections: A working manual*. US Government Printing Office, Washington, 1987.
- [26] *W. R. Tobler*: Medieval distortions: The projections of ancient maps. *Annals of the Association of American Geographers* *56* (1966), 351–360. [doi](#)
- [27] *W. R. Tobler*: Numerical approaches to map projections. *Beitrag zur theoretischen Kartographie, Festschrift für Erik Amberger*, hg. Ingrid Kretschmer. Franz Deuticke, Wien, 1977, pp. 51–64.
- [28] *W. R. Tobler*: Measuring the similarity of map projections. *The American Cartographer* *13* (1986), 135–139. [doi](#)
- [29] *H. Yabe, T. Takahashi*: Factorized quasi-Newton methods for nonlinear least squares problems. *Math. Program., Ser. A* *51* (1991), 75–100. [zbl](#) [MR](#) [doi](#)
- [30] *Q. H. Yang, J. P. Snyder, W. R. Tobler*: *Map Projection Transformation. Principles and Applications*. Taylor & Francis, London, 2000. [zbl](#) [MR](#)
- [31] *W. Zhou, X. Chen*: Global convergence of a new hybrid Gauss-Newton structured BFGS method for nonlinear least squares problems. *SIAM J. Optim.* *20* (2010), 2422–2441. [zbl](#) [MR](#) [doi](#)

*Authors' addresses:* Tomáš Bayer, Faculty of Science, Charles University, Albertov 6, Praha 2, 120 78, Czech Republic, e-mail: bayertom@natur.cuni.cz; Milada Kočandřlová, Faculty of Finance and Accounting, University of Economics, nám. W. Churchilla 1938/4, Praha 3, 130 67, Czech Republic, e-mail: kocandrlova@hotmail.cz.